

THE USE OF LINEAR PROGRAMMING AS SEARCH METHOD OF IMAGES IN ELECTRICAL IMPEDANCE TOMOGRAPHY

Miguel Fernando Montoya Vallejo, montovall@gmail.com

Claudia Natalia Lara Herrera, natylara@gmail.com

Fernando Silva de Moura, fernandosmoura@gmail.com

Julio Cesar Ceballos Aya, jccaya@usp.br

Raul Gonzalez Lima, lima.raul@gmail.com

University of São Paulo, Escola Politécnica da USP, Department of Mechanical Engineering, Av. Prof. Luciano Gualberto, no. 2231 - CEP - 05508 - 900 - São Paulo - SP

Abstract. *Electrical Impedance Tomography allows to monitor the lungs under forced ventilation and it is a non invasive procedure. It uses electrical potentials of electrodes attached to the thorax, when electrical current is imposed on some electrodes. The measurements allow estimating the electrical resistivity distribution inside the thorax, which, in turn, can be related to the lungs state. The present work evaluates the use of Linear Programming (LP) as a method to search images in Electric Impedance Tomography. Linear Programming is used to solve an ill-conditioned linear system in the Sensitivity Matrix algorithm, imposing restrictions in the solution space. These restrictions reduce the solution space to a closed region, with clinical and physical meaning. The tests were performed using numerically simulated data and experimental data. The images using Linear Programming are compared to images obtained using Lower Upper Triangular Decomposition (LU Decomposition). The use of LP and restrictions of the solution space generated images with better spacial solution, better resistivity resolution and more uniform sensitivity in the center of the domain compared to the use of the LU Decomposition and a small regularizing term*

Keywords: *Electrical Impedance Tomography, Linear Programming, Linear System*

1. INTRODUCTION

The necessity to visualize the interior of a domain whose access with devices like micro-cameras is difficult, impracticable, or impossible, led to the development of methods of estimation of images based in the variations of electric properties of the domain. Such methods are currently used in a variety of applications that involve from the control of industrial processes to the aid in medical diagnostics. Electrical Impedance Tomography (EIT) is well known among the different methods.

EIT can monitor the lungs in a continuous and non invasive way during the forced ventilation. In this technique the domain is discretized using a finite element mesh, electrodes are placed in the border of the domain, known currents are injected and electric potentials are measured through these electrodes. The electric potentials measurement makes possible to estimate the distribution of resistivity or conductivity in the interior of the domain. In medical diagnosis, EIT are being applied in different areas, such as the monitoring of cerebral blood flow and blood volume changes [9], study of cerebral haemodynamics in the newborn for many years [7] and detection and monitoring of apnea and edema [12].

Some industrial applications of the EIT are the monitoring of the solid distribution inside hidrociclone [11], images of industrial flows, volumetric flow's alterations in oil and gas [3], measures of material's distribution in two phases flows [4], images of volcanic magma [8] and detection of antitank mines [2].

In EIT, it is common to speak about the Forward Problem and Inverse Problem. In the forward problem the electric properties of the domain are defined, the currents injected and the structure of the model is known beforehand. The objective is to calculate the electric potentials in the electrodes. To calculate the electric potential in the electrodes is necessary to solve "Eq (1)"

$$[Y]\{V\} = \{C\} \quad (1)$$

where $[Y_{(\rho)}] \in \mathbb{R}^{m \times m}$ is the matrix of global rigidity in function of resistivity $\{\rho\} \in \mathbb{R}^n$ and $\{V_{(\rho)}\} \in \mathbb{R}^m$ is a matrix of corresponding voltages to each current pattern injected. The term *current pattern* is defined as the way how the current is injected, equally the term *voltage pattern* is defined as the way how the voltage is measured. In the literature, various works present different forms to inject current and to measure potentials, in the present work the patterns method *jump an electrode* was adopted.

To solve a "Eq (1)" is necessary to eliminate the singularity of the rigidity matrix, the article *Comparing reconstruction algorithms for electrical impedance tomography* [13] describes the procedure to eliminate the singularity of the rigidity matrix.

In the inverse problem the potentials in the electrodes are known as well as the currents, the structure of the model and it aims to know the electric properties distribution. For the solution of the inverse problem, exists in the literature the absolute methods and the methods that generate images of variation of the electrical properties.

For the absolute methods, the images are in absolute values of resistivity, as example it is cited topological Optimiza-

tion Method [6], The Newton Raphson Method [1] and variants of the Filter of Kalman [10]. In the methods that generate images of variation of the electric properties, the images are the difference between two values of absolute resistivities, or either, the equivalent to an absolute value in a reference system whose zero has been translated to any chosen point as zero, as an example is cited Sensitivity Matrix method which is implemented in the present work.

Variations of the resistivity distribution are the result of the solution of a linear system of the type $[A]\{x\} = \{b\}$. The objective of the present work is to evaluate the performance of the Linear Programming (LP) in the solution of the linear system, from the point of view of numerical errors propagation and the easiness to restrict the solution to the region of interest.

This paper is organized as follows, in section II the mathematical formulation of the domain is presented, also the modeling of the domain and the electrodes by means of the Finite Elements Method (FEM). In section III Sensitivity Matrix is described which is implemented to solve the inverse problem. The use of the Linear Programming in EIT and the implementation of this technique in the Sensitivity Matrix is shown in section IV. In section V it is explained the data utilized for testing LP. The results with the different generated data are shown in section VI and finishing in section VII the results are discussed.

2. Finite Element Model

Having a domain with unknown electric properties, EIT allows estimate his distribution of resistivity, given the excitation of the system consisting in current imposed in the contour of the domain and the electrical potentials are measured in regions of the contour of the domain. It is known that different tissues of the human body have different electrical properties, the relations that govern the iterations between the electricity and the magnetism are summarized in the Maxwell's equations.

The Maxwell's equations can be simplified in the following elliptic partial differential equation:

$$\nabla \cdot \left(\frac{1}{\rho} \nabla V \right) = 0 \quad \text{in } \Omega \quad (2)$$

where ρ is the electrical resistivity, V is the electrical potential and Ω is the domain in study. The "Eq (2)" is also known as forward problem, the solution of this equation determines the electrical potentials that are used in the implementation of the algorithms. The solution of the forward problem can be determined with the knowledge of the conditions of Neumann and Dirichlet on the surface of the domain $\partial\Omega$. To be able to apply the conditions of Neumann and Dirichlet the domain Ω was discretized using the finite elements method (FEM).

The domain of interest Ω is discretized in a mesh of m nodes and n triangular elements (triangular elements of three nodes), the electrical potential in each element is approximated by a function of linear interpolation that depends on the electric potential values on nodes of the element. The electric potential is described by a finite dimensional space and the problem of finding the nodal electric potentials, $\{V\}$, turns into an algebraic problem or the following linear system of equations: where $\{V\}$ is the vector of nodal electric potentials, $\{I\}$ is the vector of nodal electric currents and $[K]$ is the matrix of global rigidity in function of electrical resistivity. With the electrodes placed in the surface of the domain, the effect of the contact impedances electrode-skin must be taken into account. In this work, we considered the complete electrode model [5] to represent these effects. The considered model generates a matrix $[Y_i^e]$ and a vector Ie correspondent to each electrode placed in the surface of the domain $\partial\Omega$, the new matrix and the new vector are added in $[K]$ and $\{I\}$, respectively. The matrix $[Y_i^e]$ is

$$[Y_i^e] = \frac{ab}{3t\rho} \begin{bmatrix} 1 & \frac{1}{2} & 0 & -\frac{3}{2} \\ sim & 2 & \frac{1}{2} & -3 \\ & & 1 & -\frac{3}{2} \\ & & & 6 \end{bmatrix} \quad (3)$$

It is assumed that the potential in the metallic part of the electrode is equal, the thickness of the interface of the electrode t is smaller that the width of the electrode a ($t \ll a$).

Adding the matrix of the electrode model in the matrix of global rigidity, we obtain the following system: (1)", we obtain the following system:

$$[K_T]\{V_T\} = \{I_T\} \quad (4)$$

Once the electric potential of a reference node is chosen, the system can be solved for the vector $\{V_T\}$, a non-linear function of the resistivity distribution.

3. Sensitivity Matrix

A domain Ω that represents a distribution resistivity not-uniform $\rho(x, y)$ is discretized using FEM. Under these hypotheses, it can define the transformation $h_j : (\rho, I) \longrightarrow \{v_j\}$ for vector $\{v_j\}$ (vector of nodal electrical potentials for which current pattern), $j = 1, \dots, p$ (p number of current patterns)

$$\{v_j(\rho)\} = h_j(\rho) = [Y(\rho)]^{-1}\{I_j\} \quad (5)$$

where $\{I_j\} \in \mathbb{R}^m$ is the current pattern injected.

From the "Eq. (5)", can be concluded that the vectors of nodal voltages are nonlinear functions of the distribution of resistivity in the domain. Applying series of Taylor and truncating the series from the linear term and around a distribution ρ_0 , we obtain:

$$\{v_j(\rho)\} \approx \{v_j(\rho_0)\} + \frac{\partial h_j |_{(\rho_0)}}{\partial \rho} [\rho - \rho_0] \implies \underbrace{\{v_j(\rho)\} - \{v_j(\rho_0)\}}_{\{\Delta V\}} = \underbrace{\frac{\partial h_j |_{(\rho_0)}}{\partial \rho}}_{H_j} \underbrace{[\rho - \rho_0]}_{\{\Delta \rho\}} \quad (6)$$

Calculating the partial derivative of the transformation h_j with respect the resistivity of each element for

$$H_j(\rho_0) = \frac{\partial h_j |_{(\rho_0)}}{\partial \rho} = -[Y]^{-1} \frac{\partial [Y]}{\partial \rho} [Y]^{-1} [I_j] \quad (7)$$

$$H_j(\rho_0) = \left[-[Y]^{-1} \frac{\partial [Y]}{\partial \rho_1} [Y]^{-1} \{I_j\} \quad -[Y]^{-1} \frac{\partial [Y]}{\partial \rho_2} [Y]^{-1} \{I_j\} \quad \dots \quad -[Y]^{-1} \frac{\partial [Y]}{\partial \rho_n} [Y]^{-1} \{I_j\} \right], j = 1, \dots, p \quad (8)$$

where $[H_j] \in \mathbb{R}^{p \times n}$ is called *Sensitivity Matrix*,

To find the resistivity from the equation "Eq (7)" it is necessary to define the following performance index

$$IP = \frac{1}{2} \left([H] |_{\rho_0} \{ \Delta \rho \} - \{ \Delta V_m \} \right)^T \left([H] |_{\rho_0} \{ \Delta \rho \} - \{ \Delta V_m \} \right) + \alpha \{ \Delta \rho \}^T [F]^T [F] \{ \Delta \rho \} \quad (9)$$

where $[F] \in \mathbb{R}^n$ is a regularization matrix and α is a regularization parameter. It is necessary to determine the resistivity variation that minimizes the difference between the measured voltage and the calculated voltage, for such objective is necessary derived the performance index with respect $\{ \Delta \rho \}$ and to equal to zero

$$\frac{\partial IP}{\partial \Delta \rho} = 0 \implies [H] |_{\rho_0}^T \left([H] |_{\rho_0} \{ \Delta \rho \} - \{ \Delta V_m \} \right) + \alpha [F]^T [F] \{ \Delta \rho \} = 0 \quad (10)$$

Grouping terms in the "Eq (10)" we obtain the expression of interest

$$\left([H] |_{\rho_0}^T [H] |_{\rho_0} + \alpha [F]^T [F] \right) \{ \Delta \rho \} = [H] |_{\rho_0}^T \{ \Delta V_m \} \quad (11)$$

4. Using Linear Programming to Electrical Impedance Tomography

Linear Programming (LP) is used in TIE in the solution of linear systems of the type $[A] \{ \vec{x} \} = \{ b \}$ taking advantage of the fact that it is possible to impose restrictions in the variables $\{ \vec{x} \}$.

The problem of identifying the resistivity distributions inside of the thorax has natural restrictions, resistivity cannot be negative and cannot exceed a characteristic maximum value of a biological tissue. These restrictions become the convex space solution, simplifying the solution of the inverse problem.

To solve the linear system is necessary to rewrite the classic LP problem. An arbitrary vector is chosen $\{ \vec{x}_0 \} \in \mathbb{R}^n$ and then is proceeded to determine the vector $\{ \vec{e} \} \in \mathbb{R}^n$ as $\{ \vec{e} \} = [A] \{ \vec{x}_0 \} - \{ b \}$.

The original system of restrictions in the form $[A] \{ \vec{x} \} = \{ b \}$ is rewritten as presented in the following equation

$$[A] \{ \vec{x} \} - \{ b \} + \delta \{ \vec{e} \} = 0 \quad (12)$$

The original problem is reformulated of the following form form

$$\begin{aligned}
 & \text{Minimize} \quad \delta \\
 & \text{Subject to} \\
 & [A]\{\bar{x}\} - \{b\} + \delta\{\bar{e}\} = 0 \\
 & \{\bar{x}_{min}\} \leq \{\bar{x}\} \leq \{\bar{x}_{max}\} \\
 & 0 \leq \delta \leq \epsilon
 \end{aligned} \tag{13}$$

when $\delta \approx 0$, the solution vector $\{\bar{x}\}$ satisfies $[A]\{\bar{x}\} = \{b\}$.

Examining the "Eq (11)", it represents a linear system in the form $[A]\{x\} = \{b\}$, then by comparison we can identify our matrix $[A]$ and vectors $\{x\}$ and $\{b\}$

$$[A]\{x\} = \{b\} \implies \underbrace{\left([H]_{|\rho_0}^T [H]_{|\rho_0} + \alpha [F]^T [F] \right)}_{[A]} \underbrace{\{\Delta\rho\}}_{\{x\}} = \underbrace{\left([H]_{|\rho_0}^T \{\Delta V_m\} \right)}_{\{b\}} \tag{14}$$

Applying the previously mentioned procedure for the Sensitivity Matrix, we obtain

$$\begin{aligned}
 & \text{Minimizar} \quad \delta \\
 & \text{Sujeito a} \\
 & \left([H]_{|\rho_0}^T [H]_{|\rho_0} + \alpha [F]^T [F] \right) \{\Delta\rho\} - \left([H]_{|\rho_0}^T \{\Delta V_m\} \right) + \delta\{\bar{e}\} = 0 \\
 & \Delta\rho_{min} \leq \Delta\rho \leq \Delta\rho_{max} \\
 & 0 \leq \delta \leq \epsilon
 \end{aligned} \tag{15}$$

Where

$$\{\bar{e}\} = \left([H]_{|\rho_0}^T [H]_{|\rho_0} + \alpha [F]^T [F] \right) \{\Delta\rho_a\} - \left([H]_{|\rho_0}^T \{\Delta V_m\} \right)$$

The imposition of limits in the "Eq (14)" is having in account a prior information, the value of resistivity found for the algorithm has that to be positive for the case of tank and the object, then the value zero is fixed for the inferior limit and the value for the superior limit can be fixed for the maximum value of resistivity that can be found, for ours study case this value is the resistivity of the object. For medical applications, the resistivities inside the thorax [14], they are positive values that vary since $4\Omega m$ for the heart (muscle) even $1 \times 10^5 \Omega m$ for the present air in the lungs. Leaving of this known information as a prior, is possible to impose the limits in the variable to get medical images.

5. Simulated and Experimental data

The numerical phantom used to generate the simulated data consists of a circular domain with a 2D mesh. The resistivity distribution is known as a prior. Two sets of data are generated, one set will be called *basal* and the other set will be called *with-object*. To generate the *basal* set of simulated electrical potentials, the resistivity distribution is uniform. To generate the set *with-object* of simulated electrical potentials, the resistivity distribution of the domain is uniform except for a cylindrical region, called object, that has a higher resistivity.

The experimental data was obtained from a cylindrical container with 30 electrodes attached to its boundary with 35 mm high and 10mm wide (the thickness of each electrode is not necessary for the algorithm). The electrodes are equally spaced along the container's boundary, which was filled up to 35 mm with a $0.3g/L$ saline solution (NaCl). Its resistivity is approximately $17\Omega m$. The inner diameter of the container is $300mm$. The object, a glass cillinder, has $32mm$ of diameter and resistivity close to $10^6 \Omega m$.

To obtain the electrical potentials in the electrodes, a pair of them was electrically excited following the current pattern seen in the section 1. Then, the relative potentials were measured, except for those which share current carrying electrodes, due to hardware limitations. The pair of electrodes used for current injection was successively changed until a satisfactory number of observations was obtained, providing the necessary data for the estimation of an image. Thirty current patterns were applied.

6. Results

To obtain the simulated data it was used a phantom with uniform resistivity in a cylindrical domain and a cylindrical inclusion placed in two different positions. The first position of the object is $0.11m$ off the center "Fig.1(a) " and the second position of the object is at the center of domain "Fig.1(b) ". The resistivity of the object was $100\Omega m$. The other

elements of the domain had $10\Omega m$ of resistivity. The initial estimate of resistivity was $10\Omega m$ for the elements and the initial electrode parameters were $0,02\Omega m^2$. The injected current was $2mA$. The meshes to solve the inverse problems are shown in "Fig.2(b) and "Fig.3(b) ". The meshes to solve the direct problems are shown in "Fig.2(a) " and "Fig.3(a) ".

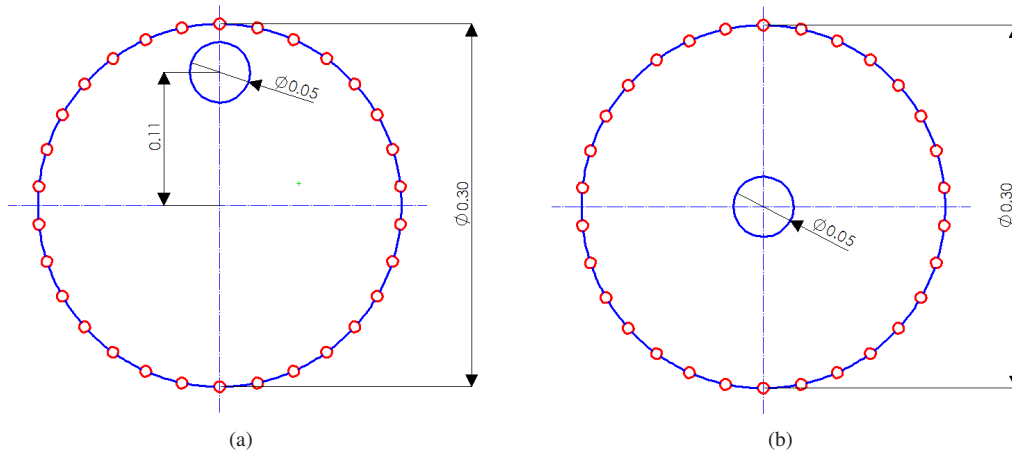


Figure 1. Object located at (a) the boundary (b) the center

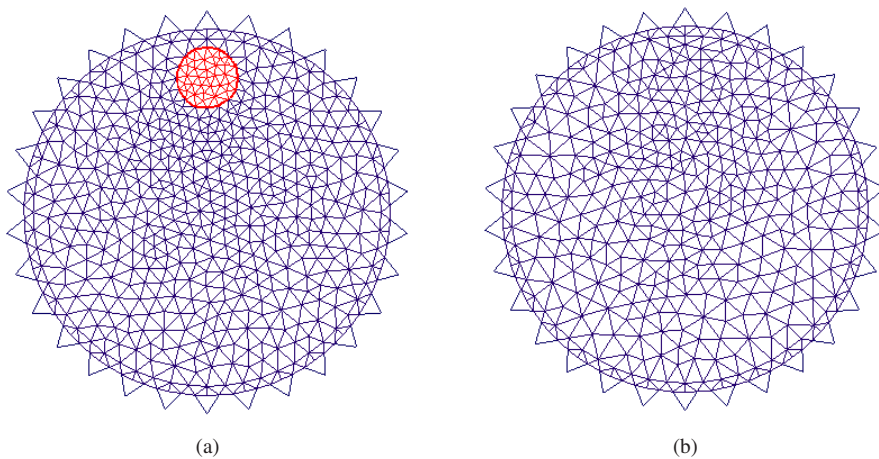


Figure 2. Finite elements meshes to solve the (a) forward and (b) inverse problem, inclusion close to the boundary

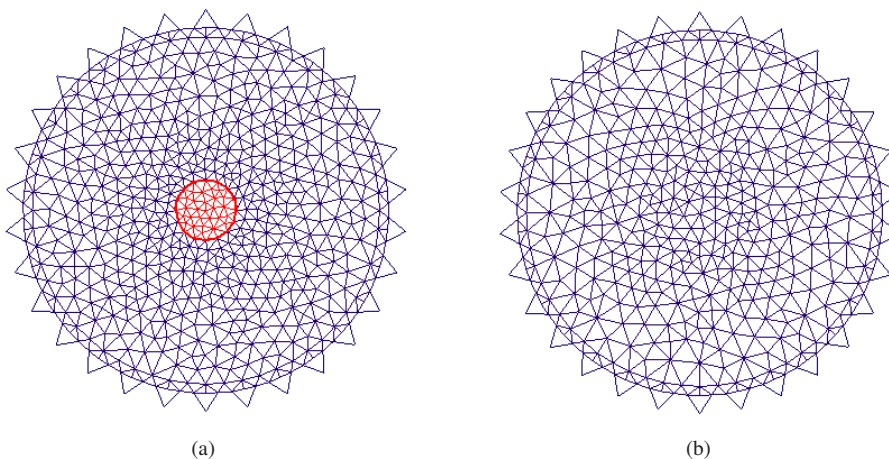


Figure 3. Finite elements meshes to solve the (a) forward and (b) inverse problem, inclusion close to the center

To obtain experimental data, the object was located in two positions, near the border and in the center of the cylindrical

vessel. The adopted electrode parameters were $0.02\Omega m^2$ and the initial resistivity of the saline solution was $20.0\Omega m$. The injected current was $2mA$ peak in amplitude and $125kHz$ in frequency. The finite elements mesh used to solve the inverse problem is shown in the "Fig.4 "

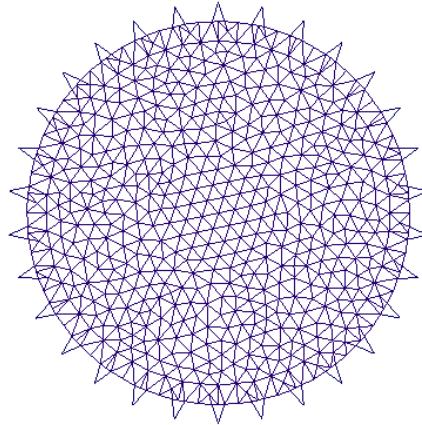


Figure 4. Finite elements mesh to solve the inverse problem with experimental data

The images obtained using simulated data are in figure 6 and figure 6. The regularization parameter was $\alpha = 1.0e^{-2}$ when the object is $0.11m$ off the center and $\alpha = 1.0e^{-2}$ when the object is at the center.

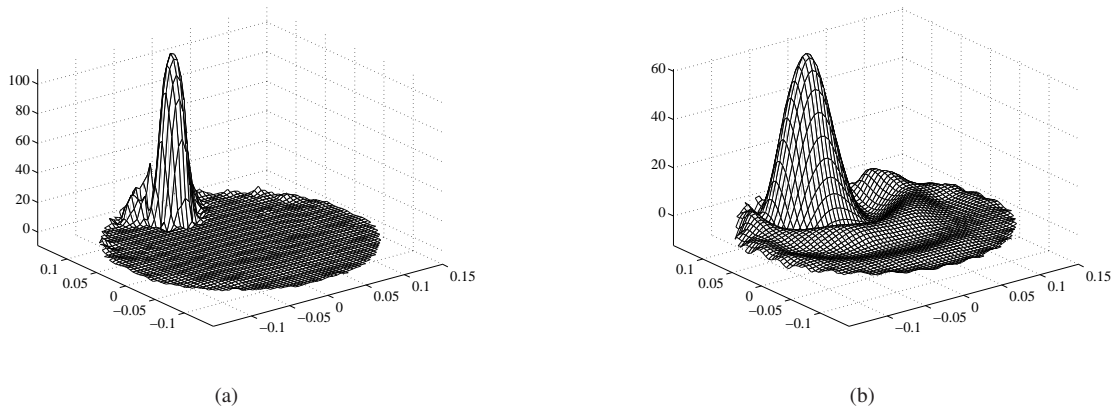


Figure 5. Variation of resistivity when the object is $0.11m$ off the center of the domain, units in $\Delta\rho[\Omega m]$, and $\alpha = 1.0e^{-2}$ (a) with LP and (b) LU Decomposition

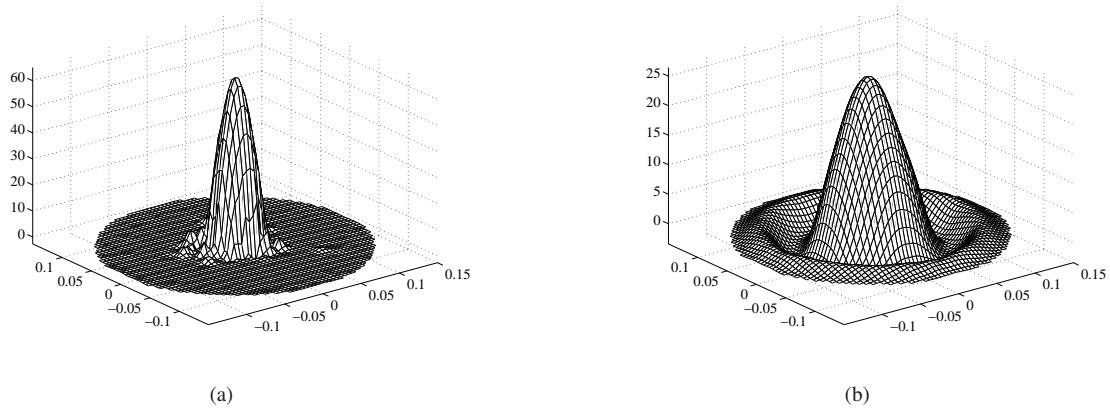


Figure 6. Variation of resistivity when the object is at the center of the domain, units in $\Delta\rho[\Omega m]$, and $\alpha = 1.0e^{-2}$ (a) with LP and (b) LU Decomposition

The images obtained using experimental data are shown in figure 6 and 6. The regularization parameter was $\alpha = 1.0e^{-3}$ when the object is 0.11m off the center and $\alpha = 1.0e^{-2}$ when the object is at the center.

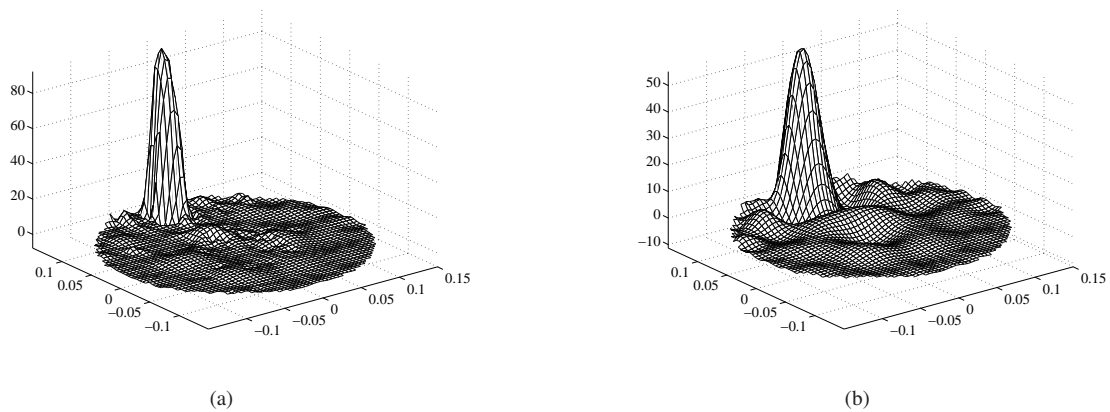


Figure 7. Variation of resistivity when the object is 0.11m off the center of the domain $\Delta\rho[\Omega m]$ and $\alpha = 1.0e^{-3}$ (a) with LP and (b) LU Decomposition

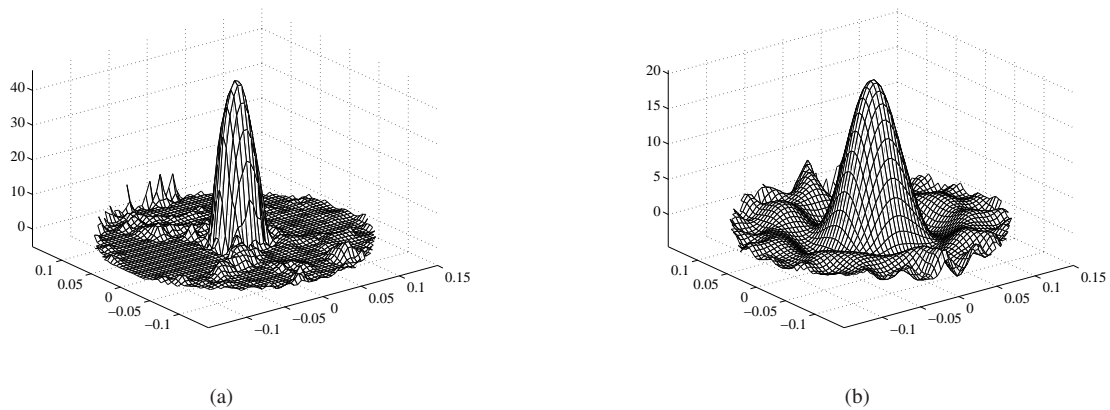


Figure 8. Variation of resistivity in the center of the tank $\Delta\rho[\Omega m]$ and $\alpha = 1.0e^{-3}$ (a) with LP and (b) LU Decomposition

The resistivity of the saline is expected to be near $20\Omega m$ for the tests with experimental data. The resistivity of the object was estimated 20% lower than the expected resistivity when the object is close to the boundary.

7. Final Comments

The image obtained using Linear Programming to solve the linear system presented higher resistivity distribution, higher resolution in space, with a satisfactory diameter and good position of the object. The image obtained using LU Decomposition and Tikhonov regularization to solve the linear system presented smaller resistivity distribution and smaller spatial resolution than using Linear Programming.

The improvement of the images using LP is partially due to the imposition of restrictions in the variables that reduce the solution space, without using a laplacian regularizing term, which penalizes high frequency spatial content. Another reason for improvement of the images using LP is the smaller numerical error propagation during the computation of the solution of linear systems.

8. Acknowledgment

The authors are grateful for the financial support from The State of São Paulo Research Foundation, through a master's scholarship, FAPESP number 04/11159-1, the financial support under FAPESP number 01/05303-4 and from The Brazilian National Research Council for a master's scholarship number CNPq number 134991/2005-2.

9. REFERENCES

- Aruca, D., 2002, "Algoritmo de Tomografia por impedância elétrica", Dissertação (Mestrado), Departamento de Engenharia Mecânica, Escola Politécnica, Universidade de São Paulo.
- Church, P.M., Philip, M.W, Stephane, G. and John, M., "Performance Assessment of an Electrical Impedance Tomography Detector for Mine-Like Objects", Defence Research Establishment Suffield DRES.
- Fehmers, G., 2003, "Volumetric flow rates from impedance tomography in oil/gas flows", 3rd World Congress on Industrial Process Tomography.
- George, D.L., Torczynski, J.R., Shollenberger, K.A., Ohern T.J. and Ceccio, S.L., 2000, "Validation of electrical-impedance tomography for measurements of material distribution in two-phase flows", International Journal of Multiphase Flow.
- Hua, J.W.P, Webster, J. and Tompkins, W., 1993, "Finite element modeling of electrode-skin contact impedance in electrical impedance", IEEE Transactions on Biomedical Engineering, Vol.40, No. 4, pp. 335-343.
- Lima, C., Silva, E. and Lima, R., 2003, "Topology optimization method applied to obtain images from electrical impedance tomography technique", Proceedings of 17th International Conference of Mechanical Engineering, pp. 535-538.
- Murphy, D., Burton, P., Coombs, R., Tarassenko, L. and Rolfe, P., 1987, "Impedance imaging in the newborn", Clin. Phys. Physiol. Meas.
- Myer, D., Constable, S. and Key, K., "Electrical Impedance Tomography of a Seafloor Volcano".
- Tidswell, T., Gibson, A., Bayford, R.H. and Holder, D.S., 2001, "Three dimensional electrical impedance tomography of human brain activity", Neuroimage.
- Trigo, F., 2001, "Filtro estendido de Kalman aplicado à tomografia por impedância elétrica", Dissertação (Mestrado), Departamento de Engenharia Mecânica, Escola Politécnica, Universidade de São Paulo.
- Williams, R.A., Dickin, F.J., Gutiérrez, J.A., Dyakowski, T. and Beck, M.S., 1997, "Using electrical impedance tomography for controlling hydrocyclohe underflow discharge", Control Engineering Practice.
- Woo, E.J., Hua, P., Webster, J.G. and Tompkins, W., 1992, "Measuring lung resistivity using electrical impedance tomography", IEEE Transactions on Biomedical Engineering, Vol.39, No. 7, pp. 756-760.
- Yorkey, T.J. and Webster, J.G., 1987, "Comparing reconstruction algorithms for electrical impedance tomography", Transactions on Biomedical Engineering, Vol.34, No.11, pp. 843-852.
- Zhang, J. and Patterson, R.P., 2006, "EIT images of ventilation: what contributes to the resistivity changes ?", Institute of Physics Publishing.

10. Responsibility notice

The author(s) is (are) the only responsible for the printed material included in this paper